Taylor & Francis
Taylor & Francis Group

Modelling, analysis and calculation of cerebral hemodynamics

SILVIA DAUN†* and THORSTEN TJARDES‡

†Department of Mathematics, University of Pittsburgh, 301 Thackeray Hall, Pittsburgh, PA 15260, USA
‡Department of Trauma and Orthopaedic Surgery, Merheim Medical Center, University of Witten-Herdecke,
Ostmerheimerstr. 200, D-51109 Cologne, Germany

Mathematical models of cerebral hemodynamics, applicable to humans and rats have been developed and analysed with the purpose of reaching a deeper insight to which degree experimental results on rats can be extrapolated to humans and to clinical management of patients. These models include regulation mechanisms involving the small cerebral arteries and arterioles, flow autoregulation, as well as CO_2 and NO reactivity. Bifurcation analysis was conducted on both models.

The human model includes Hopf-bifurcations, which allow for the existence of periodic solutions with a time scale comparable to Lundberg's plateau waves in intracranial pressure (P_{ic}). By contrast, the rat model does not manifest Hopf-bifurcations and thus does not predict the existence of periodic solutions with critical high P_{ic}.

Therefore the model questions the relevance of rodent injury models to predict human physiology following TBI.

Keywords: Cerebral hemodynamics; Regulation mechanisms; Mathematical modelling; Plateau waves

AMS Subject Classification: 37G15; 37N25; 81T80; 93A30

1. Introduction

Elevation of intracranial pressure is a phenomenon that accompanies many diseases. While a slow, *i.e.* chronic, elevation of intracranial pressure is often tolerated for a long time without significant clinical symptoms, acute elevation of intracranial pressure cannot be compensated. For instance traumatic brain injury (TBI) is typically accompanied by intracranial hypertension. This may be due to intracranial haemorrhage, which often is amenable to surgical treatment. More often there is diffuse tissue damage resulting in brain edema. In contrast to localized haemorrhage diffuse swelling of the brain cannot be treated causally. Increased intra-cerebral pressure due to brain swelling can only be ameliorated by indirect measures. Increasing intravascular colloid osmotic pressure by infusion of high molecular weight substances, deep sedation and control of intracranial blood flow by modulation of CO_2 tension are the tools of the physician to reduce intracranial pressure. However, persistent elevation of intracranial pressure and recurrent pressure peaks are the major causes for recurrent brain damage resulting in permanent disability or

*Corresponding author. Email: dauns@upmc.edu

even brain death. Clinical research, *e.g.* testing or comparing different types of interventions, in these patients is difficult or impossible due to ethical reasons. Thus experimental research is focused on animal models of TBI. Usually rat models with either fluid percussion mechanism or a cortical impact mechanism are used. These models have improved our understanding of the cellular mechanisms of TBI [1] and are currently used to explore the therapeutic potential of stem cell transplantation [2] after TBI. With respect to the effects of clinical interventions to improve cerebral perfusion the question to what extent observations from the animal can be transferred to human injury remains unanswered.

Plateau waves consist of a sudden rapid elevation of intracranial pressure to $50-100$ mmHg for $5-20$ min, followed by a plateau. After a sustained period of elevation, termination of the wave is characterized by a rapid decrease of ICP.

These sudden increases of ICP are thought to be a source of secondary brain damage. Thus a deeper understanding of the mechanisms and dynamics resulting in the formation of plateau waves is mandatory.

We developed and analysed a human model of cerebral hemodynamics and compared these analysis results with results of the analysis of our earlier derived rat model of cerebral hemodynamics [3].

The purpose of this comparison is to evaluate whether experimental results of rats can be extrapolated to humans and finally to the clinical management of patients.

With these models TBI is simulated by (1) changing intracranial pressure (P_{ic}) linearly from 6 to 33 mmHg in the first 5 min and decreasing it linearly to 28 mmHg for 23 h 55 min, (2) decreasing arterial CO_2 pressure ($40-33$ mmHg) and increasing heart rate ($80-100$ bpm) linearly over 24 h (Waschke *et al.* [4]).

The model equations in both systems are almost the same. The only equational difference is given by the description of the interaction of the NO and the CO_2 reactivity. Both systems differ in parameters. Both models represent anatomically correct models for the particular species.

2. Qualitative model description

A work of Ursino *et al.* [5] is used as the basic model for our new investigations. The derivation of the corresponding model equations is described in detail in Ref. [3] and all model equations are given in Appendix A.

The blood flow starting from the left ventricle of the heart through the brain and back to the right ventricle of the heart is modeled by a hydraulic system of series connected vessels. The parallel blood vessels which exist after each ramification are comprised of one entire vessel.

Figure 1 shows the biomechanical analog of the mathematical model. Starting from the left ventricle a certain amount of blood, the cardiac output Q is ejected into the aorta. The first extracranial segment of the model is given by the aorta, which is represented by a hydraulic resistance R_a and a hydraulic compliance C_a. The aorta branches out into the large and middle cerebral arteries, which represent the first intracranial segment of the model. It is represented by the hydraulic resistance R_{la} and the hydraulic compliance C_{la}.

The pial arteries and arterioles compose the second intracranial segment of the model, which is described by the hydraulic resistance R_{pa} and the hydraulic compliance C_{pa}. R_{pa} and C_{pa} are regulated actively by the cerebrovascular regulation mechanisms (autoregulation, CO_2 and NO reactivity). The resistance R_{pa} is the sum of the resistances of the pial arteries and arterioles and the capillaries. To model the pial intracranial segment

Figure 1. Biomechanical analog of the mathematical model, in which resistances are represented with restrictions and compliances with bulges. P_a, systemic arterial pressure; R_a and C_a, systemic arterial resistance and compliance; Q, cardiac output from the left heart, only a fraction of it goes into head; P_{la}, R_{la} and C_{la}, pressure, resistance and compliance of large intracranial arteries, respectively; P_{pa}, R_{pa} and C_{pa}, pressure, resistance and compliance of pial arterioles, respectively; P_c, capillary pressure; q, tissue cerebral blood flow; R_{pv}, resistance of proximal cerebral veins; C_{vi}, intracranial venous compliance; P_v, cerebral venous pressure; P_{vs} and R_{vs}, sinus venous pressure and resistance of the terminal intracranial veins, respectively; q_f and q_o, cerebrospinal fluid flow into and out of the craniospinal space, respectively; R_f and R_o, inflow and outflow resistance; P_{ic} and C_{ic}, intracranial pressure and compliance, respectively; P_{cv}, central venous pressure, R_{ve} and C_{ve}, resistance and compliance of the extracranial veins.

R_{pa} was bisected and connected before and after the pial arterial compliance to get the blood flow into these arteries as well as the blood flow out of these vessels into the capillaries dependent on the regulation mechanisms.

Because the capillaries are very thin and hardly extensible vessels they were not modeled with a compliance.

The third intracranial segment consists of the venules and the small and large cerebral veins and is represented by the hydraulic resistance R_{pv} and the hydraulic compliance C_{vi}. The last intracranial segment represents the terminal intracranial veins (*e.g.* lateral lakes, bridge veins). During intracranial hypertension these vessels collide or narrow at their entrance into the dural sinuses. Therefore the resistance R_{vs}, which describes these cerebral veins, is modeled by a starling resistor (cf. [6]).

The compliance of the intracranial space is given by C_{ic}.

The last segment of the model represents the vena cava, which transports the blood back into the heart again. It is described by the hydraulic resistance R_{ve} and the hydraulic compliance C_{ve}.

A formation of cerebral edema is modeled by wateroutflow q_f at the capillaries into the craniospinal space and reabsorption q_o at the dural sinus. The strength of cerebral edema is regulated by the inflow resistance R_f and the outflow resistance R_o.

The differential equations which describe the pressure changes in each segment of the model are derived from the biomechanical analog.

Cerebrovascular regulation mechanisms work by modifying the resistance R_{pa} and the compliance C_{pa} (and hence the blood volume and the blood flow) in the pial arterial–arteriolar vasculature.
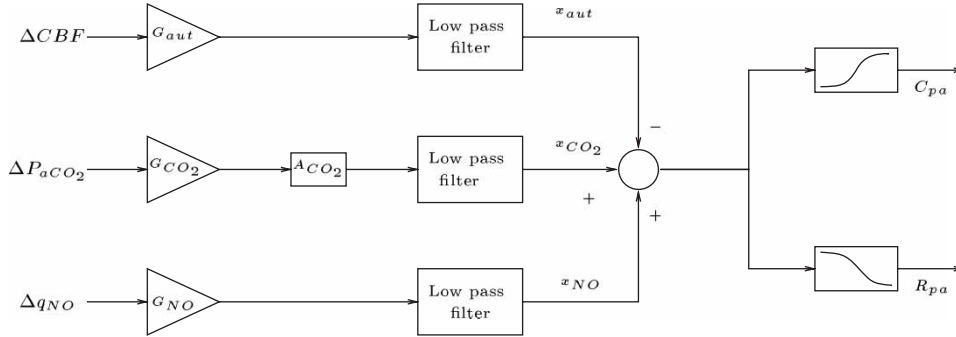
Figure 2. Block diagram describing the action of cerebrovascular regulation mechanisms according to the present model. The upper branch describes autoregulation, the middle branch indicates CO_2 response, and the lower branch describes NO reactivity. The input quantity for autoregulation is cerebral blood flow change ($\Delta CBF = ((q - q_n)/q_n)$). The input quantities for the CO_2 and NO mechanisms are the logarithm of arterial CO_2 tension (P_aCO_2), *i.e.* $\Delta P_{aCO_2} = \log_{10}(P_{aCO_2}/P_{aCO_2 n})$, and the logarithm of NO production (q_{NO}), *i.e.* $\Delta q_{NO} = \log_{10}(q_{NO}/q_{NO n})$, respectively. The dynamics of these mechanisms are simulated by means of a gain factor (G) and a first order low pass filter with time constant τ. The variables x_{aut}, x_{CO_2} and x_{NO} are three state variables of the model that account for the effect of autoregulation, CO_2 reactivity and NO reactivity, respectively, they are given in ml/mmHg. q_n, $P_{aCO_2 n}$ and $q_{NO n}$ are set points for the regulatory mechanisms. The gain factor of the CO_2 reactivity is multiplied by a corrective factor A_{CO_2}, because as a consequence of tissue ischemia CO_2 reactivity is depressed at low CBF levels. These three mechanisms interact nonlinearly through a sigmoidal static relationship, and therefore producing changes in pial arterial compliance and resistance.

There are three of these mechanisms considered inside the model, the autoregulation, the CO_2 and the NO reactivity.

The block diagram in figure 2 describes the action of cerebrovascular regulation mechanisms according to the present model. They are modeled by means of a first order low pass filter with time constant τ and gain G.

These three mechanisms interact nonlinearly through a sigmoidal static relationship, and therefore producing changes in pial arterial compliance and resistance.

The last mechanism which is included into the model desribes the release of norepinephrine into blood during sympathetic nerve stimulation. Cardiac function is modulated in many aspects by norepinephrine. Among the primary effects of this substance is an increase in heart rate and thus an increase in cardiac output Q. A detailed description of this mechanism can be found in Ref. [3].

3. Rat model

The estimation of systemic parameters of the rat model under basal conditions is described now. The values of the compliances in the craniospinal space, like C_{la}, C_{pa} and C_{vi}, and the intracranial compliance C_{ic} were fitted by using pressure curves of these compartments. The values were fitted in the way that the model amplitudes of the pressures in each compartment are equal to the given physiological amplitudes of the pressures (see [7–10]).

The basal value of the resistance of the large intracranial arteries is calculated by using the Hagen–Poiseuille law $R = (8\eta l)/(r^4 \pi)$. All other model resistances, R_s, R_{pa}, R_{pv}, R_{vs} and R_{ve} are calculated by using the mean pressure values in each compartment (see [7–9]) and solving the differential equations describing the system in steady state. All rat model parameters under basal conditions are given in table 1.

Table 1. Basal values of rat model parameters.

$C_a = 0.0042$ ml/mmHg	$R_s = 99.4286$ mmHg s ml^{-1}
$n = 13$	$b = 378/60$ beats s$^-$
$\nu = 0.1852$ ml per beat	$k_{Cla} = 0.0305$ ml
$R_{la} = 47.1609$ mmHg s ml^{-1}	$k_R = 1.6258e + 06$ mmHg^3 s ml^{-1}
$C_{pan} = 4.7277e - 07$ ml/mmHg	$\Delta C_{pa1} = 6.6188e - 06$ ml/mmHg
$\Delta C_{pa2} = 3.7822e - 07$ ml/mmHg	$R_{pv} = 29.4756$ mmHg s ml^{-1}
$R_f = 2830$ mmHg s ml^{-1}	$R_o = 1783$ mmHg s ml^{-1}
$q_n = 0.1696$ ml s^{-1}	$\tau_{aut} = 20$ s
$G_{aut} = 0.00006$ ml/mmHg	$\tau_{CO_2} = 50$ s
$G_{CO_2} = 0.000435$ ml/mmHg	$P_{aCO_2}n = 33$ mmHg
$\tau_{NO} = 40$ s	$G_{NO} = 0.000125$ ml/mmHg
$q_{NOn} = 54.1$ ng/g tissue	$k_{CO_2} = 27$
$b_{CO_2} = 19$	$k_{ven} = 4.9353e - 08$ ml
$P_{cv} = 1.7$ mmHg	$R_{vs1} = 5.566$ mmHg s ml^{-1}
$P_{v1} = -2.5$ mmHg	$R_{ve} = 2.9476$ mmHg s ml^{-1}
$k_E = 41$ ml^{-1}	$\Delta hr_{max} = 175/60$ beats s$^-$
$\tau_{hr} = 5$ s	$k_{NE} = 100$ µg kg^{-1} min

Numerical simulations using these model parameters and validations of the rat model have been shown in Ref. [3]. In particular, in this paper pathological cases of serious injuries have been simulated by modifying corresponding model parameters.

4. Human model

The overall aim of our work was to develop and analyse a rat model as well as a human model of cerebral hemodynamics with the purpose of reaching a deeper insight into whether experimental results on rats can be extrapolated to humans and to clinical management of patients.

In this section the parameters of the developed model equations in Ref. [3] will be determined to get a model which describes the human cerebral hemodynamic realistically.

The only difference between the human and the rat model described in Ref. [3], besides the different set of parameters, consists of the relation between the NO and CO_2 reactivity, which in the case of the rat model is described by:

$$q_{NO} = 0.4332 \times P_{aCO_2} + 39.8048. \tag{1}$$

In the case of the human model there exist no reliable sources that describe an analogical dependence of the NO production rate on P_{aCO_2} or vice versa. This is the reason why the relation between q_{NO} and P_{aCO_2} is not considered in the human model.

The following sections show the results of the bifurcation analysis† of the human and the rat model. The model results are compared afterwards.

The parameters of the human model are determined or rather taken from earlier works as follows:

---

†Both model equations are analysed depending on their model parameters. A bifurcation occurs when a small smooth change made to the parameter values of a system causes a sudden qualitative change in the system's long term dynamical behaviour.

The arterial compliance C_a was chosen in the way that the diastolic and systolic pressures are 80 and 120 mmHg respectively, which means that the pressure curve of the aorta has an amplitude of 40 mmHg.

The values of the systemic arterial resistance R_s, the heart rate b and the stroke volume ν are given by Peskin *et al.* [11].

The parameter $k_{C_{la}}$ is a measure for the compliance of the large and middle cerebral arteries [$C_{la} = k_{C_{la}}/(P_{la} - P_{ic})$] and chosen in the way that the compliance under basal conditions is 0.8 ml/mmHg. McGavock *et al.* [12] measured a compliance of these cerebral arteries of 1.0 ± 0.4 ml/mmHg experimentally.

The values for the parameters, which describe the resistance of the large cerebral arteries, the compliances and resistances of the pial and the intra and extracranial vessels, as well as the autoregulation and the CO_2 reactivity in the case of a patient, are taken from works of Ursino *et al.* [5,6].

The basal value of the NO production rate is corresponding to Vaughn *et al.* [13] $6.8 \times 10^{-14}\,\mu\mathrm{mol}\,\mu\mathrm{m}^{-2}\,\mathrm{s}^{-1}$. The produced NO molecules are metabolised very quickly after production. That is the reason why the time constant for the NO mechanism τ_{NO} is chosen as one fourth of the time constant of the CO_2 reactivity τ_{CO_2}.

The parameters which describe the process of sympathetic nerve stimulation, hr_{max}, τ_{hr}, k_f and τ_{NE}, are given in a work of Mokrane *et al.* [14] for dogs. These cardiac parameters of 30–40 kg dogs are corresponding to [14] comparable to the cardiac parameters of men and therefore taken over into this system.

4.1 Simulation results

With the given data from table 2 numerical simulations were performed in this section, to show that the model reflects also a reasonable and realistic description of the cerebral perfusion of men. Pathological cases of serious head injuries have been simulated by modifying model parameters like the CSF outflow resistance R_o, CSF inflow resistance R_f, and the parameters which are relevant for blood flow regulation. The results of these simulations are given in section origin. Figures 7 and 8 show the changes in intracranial pressure by changing the above mentioned parameters.

Table 2. Basal parameter values of the human model.

|	
$C_a = 1.5$ ml/mmHg	$R_s = 1.05$ mmHg s ml^{-1}
$b = 80/60$ bps	$\nu = 70$ ml per beat
$k_{C_{la}} = 64.4$ ml	$R_{la} = 0.6$ mmHg s ml^{-1}
$k_R = 13{,}100$ mmHg^3 s ml^{-1}	$C_{pan} = 0.205$ ml/mmHg
$\Delta C_{pa1} = 2.87$ ml/mmHg	$\Delta C_{pa2} = 0.164$ ml/mmHg
$R_{pv} = 0.88$ mmHg s ml^{-1}	$R_f = 2380$ mmHg s ml^{-1}
$R_o = 526.3$ mmHg s ml^{-1}	$q_n = 12.5$ ml s^{-1}
$\tau_{aut} = 20$ s	$G_{aut} = 3$ ml/mmHg
$\tau_{CO_2} = 40$ s	$G_{CO_2} = 8$ ml/mmHg
$P_{aCO_2}n = 40$ mmHg	$\tau_{NO} = 10$ s
$G_{NO} = 5$ ml/mmHg	$q_{NOn} = 6.8 \times 10^{-14}\,\mu\mathrm{mol}\,\mu\mathrm{m}^{-2}\,\mathrm{s}^{-1}$
$k_{CO_2} = 15$	$b_{CO_2} = 0.5$
$k_{ven} = 0.155$ ml	$P_{cv} = 4$ mmHg
$R_{vs1} = 0.366$ mmHg s ml^{-1}	$P_{v1} = -2.5$ mmHg
$R_{ve} = 0.16$ mmHg s ml^{-1}	$k_E = 0.077$ ml^{-1}
$\mathrm{hr}_{max} = 72.6/60$ bps	$\tau_{hr} = 5$ s
$k_f = 1.21$ Hz	$\tau_{NE} = 9$ s
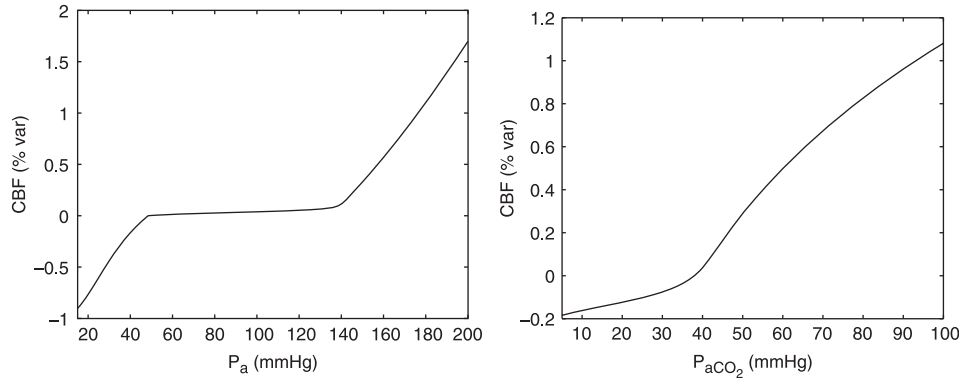
Figure 3. Regulation mechanisms of the human model. Left: Autoregulation curve, lower and upper autoregulation limits are at $P_a = 50$ and $140\,$mmHg, respectively (see [5]). Right: CO_2 Reactivity. The simulated changes in CBF because of changes in P_{aCO_2} agree with experimental data of Harper *et al.* [15].

The autoregulation curve of men, which describes the dependence of cerebral blood flow on arterial blood pressure is shown in the left of figure 3. The lower and upper autoregulation limits are 50 and 140 mmHg, respectively. These limits were also simulated and validated with experimental data by Ursino *et al.* [5].

The dependence of cerebral blood flow on arterial CO_2 pressure is shown in the right of figure 3. The simulation results correspond to the measured data of Harper *et al.* [15] and to the simulation results of Ref. [5].

The NO reactivity is shown in the left of figure 4. The simulated dependence of CBF on the NO production rate matches with a work of Kavdia *et al.* [16], who calculated the dependence of vessel diameter on the endothelial NO concentration with a mathematical model and validated their results with experimentally given data. The basal value of the NO production rate q_{NO} is $6.8 \times 10^{-14}\,\mu$mol μm^{-2} s^{-1}. Any increase in NO production yields a vasodilation of the pial vessels and an increase in cerebral blood flow, whereas any decrease in NO production yields a vasoconstriction of these vessels and a decrease in CBF.

The dependence of the CO_2 reactivity on the NO production rate is shown in the right of figure 4. One can see that, despite the neglect of a direct relation between P_{aCO_2} and q_{NO},
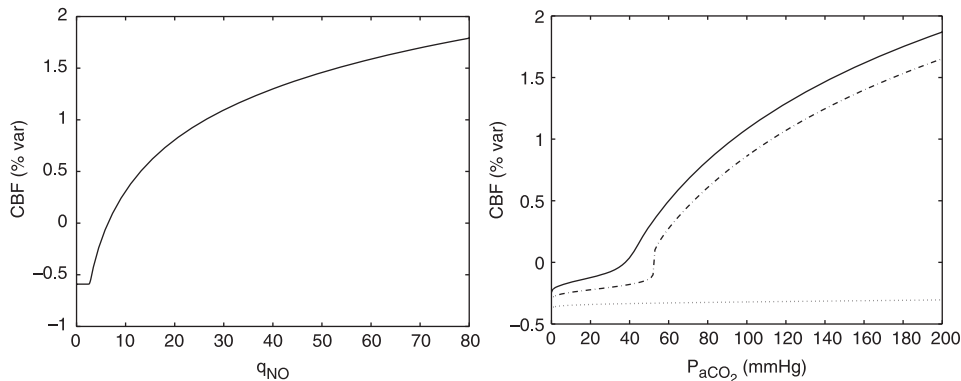
Figure 4. Left: NO reactivity. Simulated changes in CBF because of changes in the NO production rate agrees with experimental given data of Kavdia *et al.* [16]. Right: Dependence of CO_2 reactivity on the NO production rate: $q_{NO} = 6.8$ (basal value), $q_{NO} = 5$ (dashed line) and $q_{NO} = 4$ (dotted line).
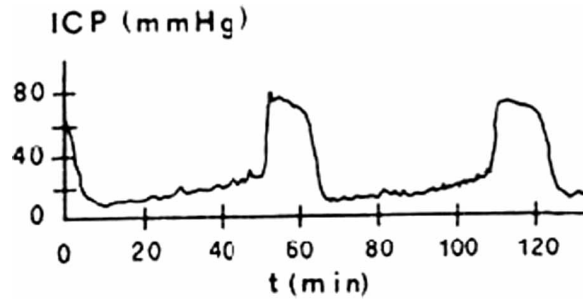
Figure 5.   Clinically observed intracranial pressure in patients with severe head injury (taken from [19,20]).
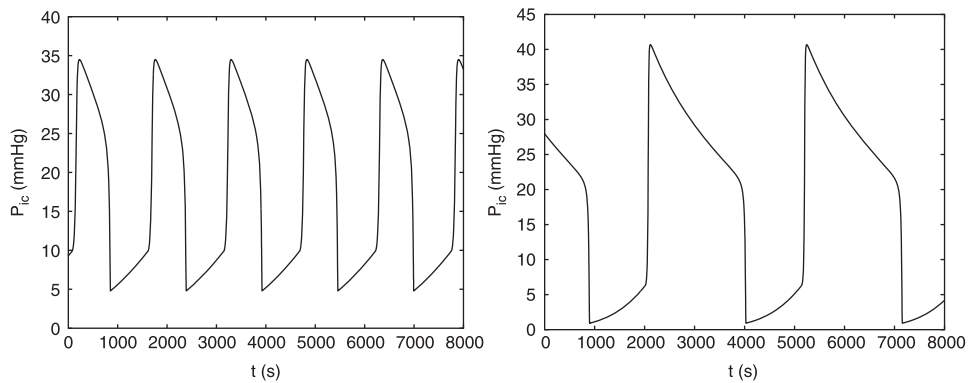

Figure 6.   Simulated intracranial plateau waves. Left: The heart rate was decreased to 75 bmp and the NO production rate and the arterial CO_2 pressure were increased to $30 \times 10^{-14} \, \mu mol \, \mu m^{-2} \, s^{-1}$ and 100 mmHg, respectively. Right: The heart rate, the NO production rate and the arterial CO_2 pressure have been raised to 89 bpm, $350 \times 10^{-14} \, \mu mol \, \mu m^{-2} \, s^{-1}$ and 50 mmHg, respectively.

the NO mechanisms have an indirect and strong impact on the CO_2 reactivity. This indirect impact is given by changes in cerebral blood flow by means of NO, which on the one hand serve as input for autoregulation and on the other hand affect the corrective factor A_{CO_2} of the CO_2 reactivity and therefore the strength of this regulation mechanism.

5. Results of the bifurcation analysis of the human model

In the human model one observes supercritical Hopf-bifurcations‡ by changing the relevant parameters belonging to the blood regulation mechanisms and to the cerebrospinal fluid flow. The periodic solutions which originate at these points have a time pattern comparable to Lundberg's A- or plateau waves.

A clinically observed intracranial plateau wave in patients with severe head injury is shown in figure 5. Figure 6 shows simulated intracranial plateau waves. In the left of figure 6 the

---

‡At a supercritical Hopf-bifurcation stable periodic solutions bifurcate from a stationary solution, which becomes unstable [17,18].

heart rate b was decreased to 75 bmp, which corresponds to a decrease in systemic blood pressure P_a to 91.9 mmHg and the NO production rate q_{NO} and the arterial CO_2 pressure P_{aCO_2} were increased to $30 \times 10^{-14} \, \mu mol \, \mu m^{-2} \, s^{-1}$ and e100 mmHg, respectively.

The heart rate, q_{NO} and P_{aCO_2} were increased to 89 bpm, which corresponds to an increasing of P_a to 109 mmHg, $350 \times 10^{-14} \, \mu mol \, \mu m^{-2} \, s^{-1}$ and 50 mmHg respectively in figure 6 on the right.

5.1 Origin of plateau waves

The analysis of our human model shows that either a vasodilatory stimulus, an increase in the CSF outflow resistance R_o, or a reduction in the CSF inflow resistance R_f cause an initiation of plateau waves in the intracranial pressure.

A vasodilatory stimulus is given by changes in the CO_2 concentration in blood, in the NO production at the endothelial cells in the vessel wall and in the blood pressure. Any increase of P_{aCO_2} or q_{NO} yields an arterial–arteriolar vasodilation with an increase in CBF as a consequence. On the other hand any decrease in P_a yields a decrease in CBF with an activation of cerebral autoregulation and arterial–arteriolar vasodilation as a consequence. The corresponding increase in arterial blood volume yields an increase in ICP.

This result is illustrated in figure 7, which shows the time pattern of ICP, where heart rate, arterial CO_2 pressure and the NO production rate have been changed linearly during integration. The heart rate b and therefore the arterial blood pressure, have been increased linearly from 68 to 88 bpm with occurrence of periodic solutions from 70.6 to 84.1 bpm (P_{aCO_2} and q_{NO} were also increased during this simulation to 100 mmHg and $30 \times 10^{-14} \, \mu mol \, \mu m^{-2} \, s^{-1}$, respectively) (top left). The arterial CO_2 pressure P_{aCO_2} has been increased linearly from 170 to 440 mmHg with occurrence of periodic solutions from 214.1 to 394.1 mmHg (top right) and the NO production rate q_{NO} has been increased linearly from 30 to $300 \times 10^{-14} \, \mu mol \, \mu m^{-2} \, s^{-1}$ with occurrence of periodic solutions from $q_{NO} = 99.6 \times 10^{-14}$ to $264.4 \times 10^{-14} \, \mu mol \, \mu m^{-2} \, s^{-1}$ (bottom). The P_{aCO_2} interval in which periodic solutions exist does not belong to a reasonable physiological range. The periodic solutions can be shifted into a reasonable physiological interval of P_{aCO_2} by, for example, increasing the NO production rate.

This result agrees with a thesis held by Rosner and Becker [21].

The analysis of the human model shows also that changes in CSF outflow and inflow resistance can initiate plateau waves. This result is illustrated in figure 8, which shows the time pattern of ICP by (a) increasing the CSF inflow resistance R_f linearly from 80 to 190 mmHg s/ml during integration with occurrence of periodic solutions from 89.95 to 154.77 mmHg s/ml (left) and (b) by increasing the CSF outflow resistance R_o linearly from 5000 to 21,000 mmHg s/ml during integration with occurrence of periodic solutions from 8093.42 to 15054.47 mmHg s/ml (right).

This result corresponds to a result given by Ursino *et al.* [19] who showed by analysing their model of cerebral hemodynamics that plateau waves, which are also ascribed to the presence of Hopf-bifurcations, can originate even without a vasodilatory stimulus, provided CSF outflow resistance is increased and intracranial compliance is reduced. Which means that the oscillations are self-sustained, *i.e.* they may occur without any external perturbation, simply as a consequence of the intrinsic instability of system dynamics.
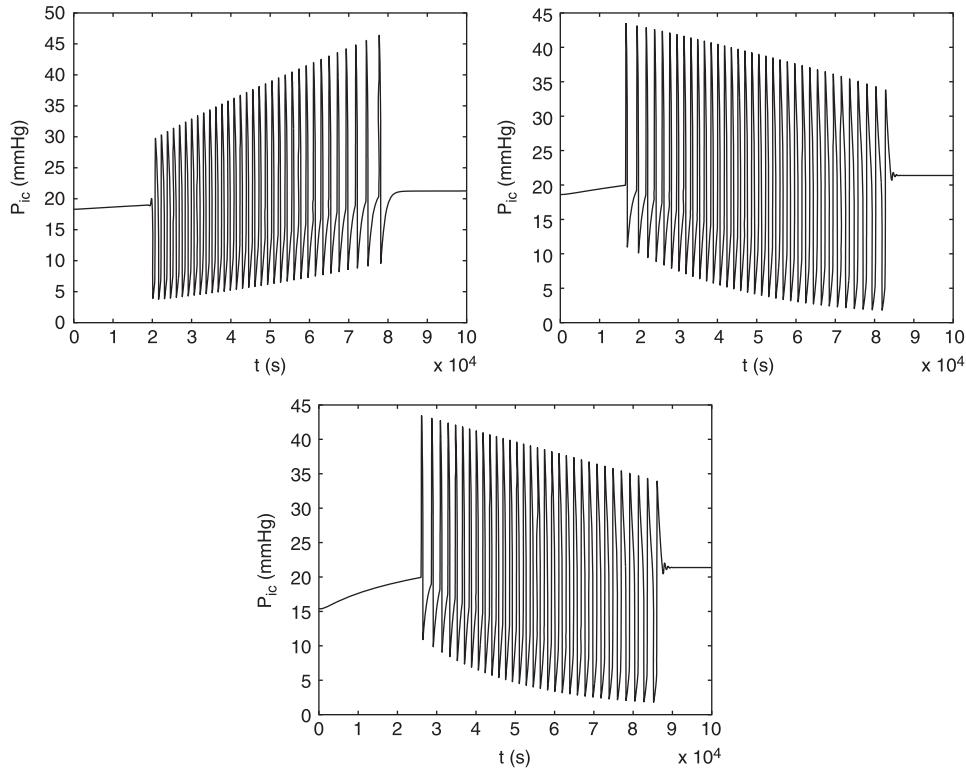
Figure 7.   Time pattern of intracranial pressure. The parameters which are relevant for the regulation mechanisms have been raised linearly during integration. In all three cases one can see an appearance and disappearance of periodic solution at specific parameter values.
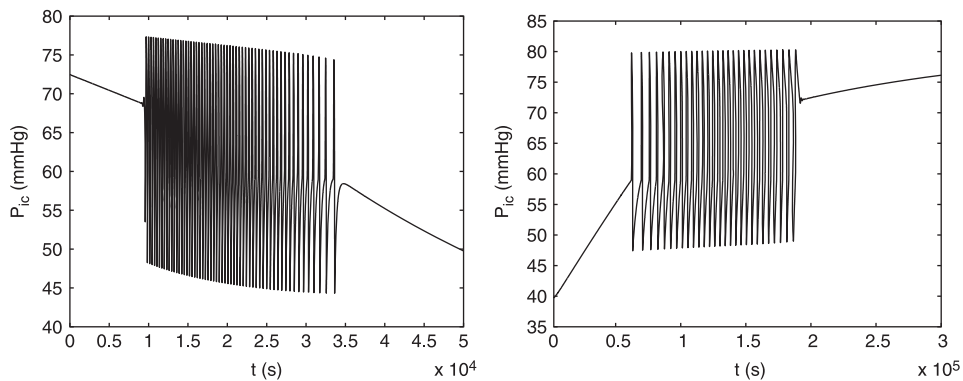

Figure 8.   Time pattern of intracranial pressure. The CSF inflow resistance R_f (left) and the CSF outflow resistance R_o (right) have been changed linearly during integration. In both cases one can see an appearance and disappearance of periodic solutions at specific parameter values.

6. Results of the analysis of the rat model

By analysing the human and the rat model we found an interesting difference in the model behaviour. The mechanism of sympathetic nerve stimulation is phenomenological comparable in both systems. In contrast one observes a totally different behaviour in the human and the rat model by changing the parameters belonging to the regulation mechanisms and by changing the parameters belonging to the CSF inflow and outflow into the craniospinal space.

Section 5 showed the existence and possible origins of plateau waves in the human model.

In contrast to that there exist no Hopf-bifurcations in the rat model.

That means no plateau waves with critical high pressure peaks arise by changing the parameters which are relevant for vessel vasodilation or by changing the parameters describing CSF flow.

These results are illustrated in figures 9 and 10.

In figure 9 the time course of intracranial pressure is given by (a) changing the heart rate b linearly from 320 to 450 bpm (P_{aCO_2} and f were also increased to 82.5 mmHg and 163 ng/g tissue, respectively) (top left), (b) changing P_{aCO_2} linearly from 30 to 450 mmHg (top right) and (c) by changing the parameter f which describes the changes in the NO production rate in the case of the rat model (see equation (1)) from 0 to 10,000 ng/g tissue (bottom) during integration. In all three cases we also observe an increase in ICP by increasing the above
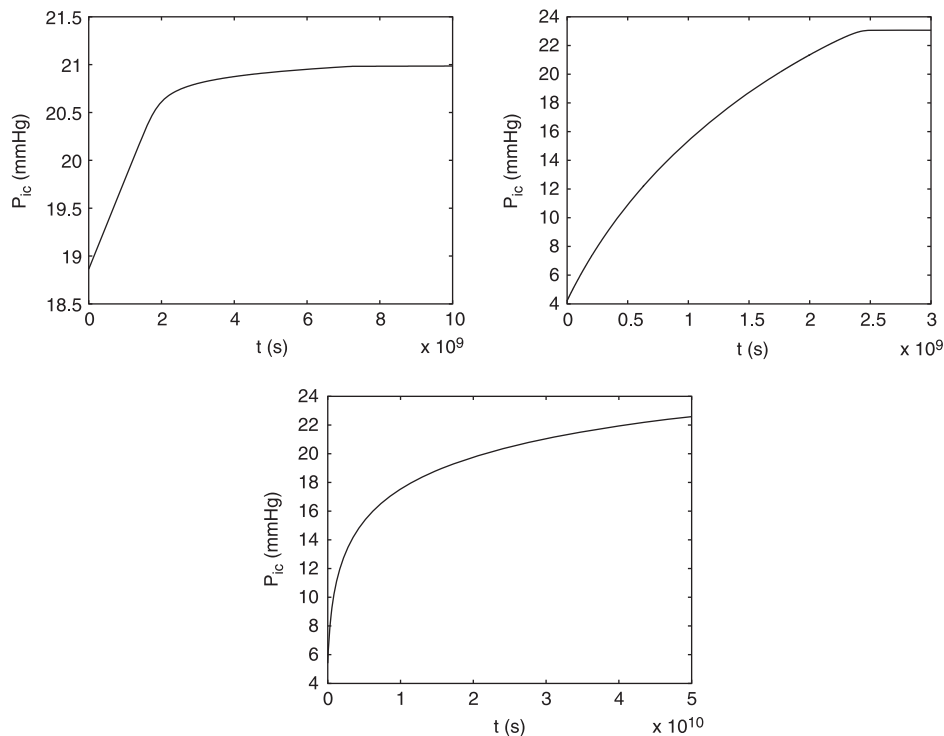

Figure 9. Time courses of intracranial pressure. The relevant parameters of the regulation mechanisms have been increased linearly during the integration. The behaviour of ICP is stationary and stable. There is no occurrence of periodic solutions.
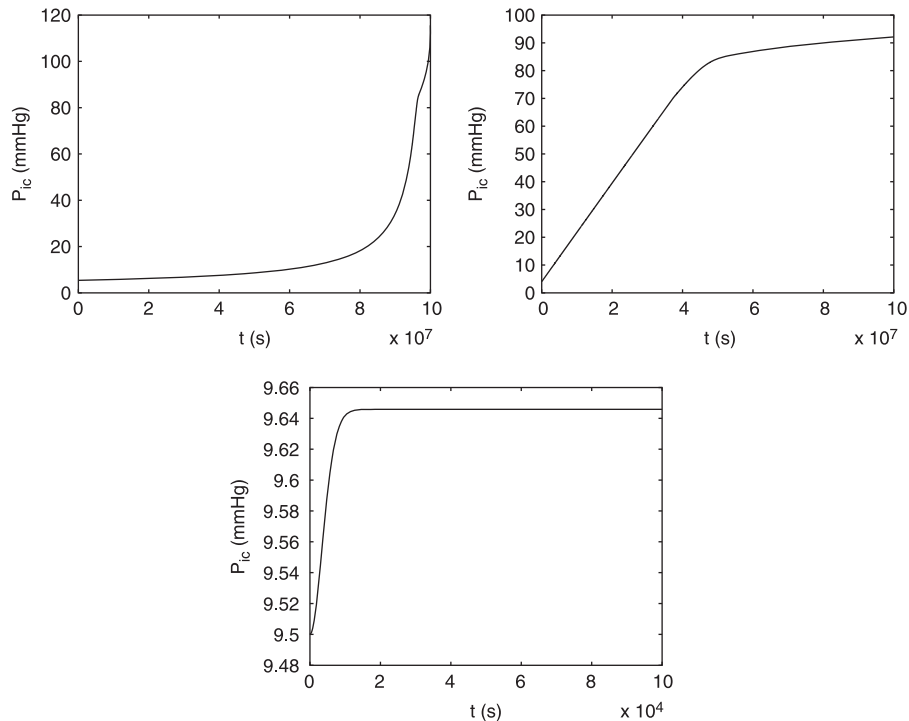
Figure 10. Time pattern of intracranial pressure simulated with the rat model. The CSF inflow resistance R_f (top left), the CSF outflow resistance R_o (top right) and the parameter k_E (bottom) which describes changes in the intracranial compliance have been changed linearly during integration. All other model parameters have not been changed. The behaviour of ICP is stationary and stable. There is no occurrence of periodic solutions.

mentioned parameters but we do not see an occurrence of periodic solutions in contrast to the human model (figure 7).

Figure 10 shows time patterns of ICP simulated with the rat model where (a) the CSF inflow resistance R_f has been decreased linearly from its basal value 2830–0.001 mmHg s/ml, (b) the CSF outflow resistance R_o has been increased linearly from 1000 to 1,00,000 mmHg s/ml and (c) the parameter k_E which describes changes in the intracranial compliance has been changed linearly from 41 to 410 l/ml during integration. In all three cases the behaviour of the intracranial pressure is stationary and stable and we do not observe an occurrence of periodic solutions in contrast to the human model (figure 8).

7. Discussion

In this paper mathematical models of cerebral hemodynamics under physiological aspects applicable to humans and rats are presented. The overall aim was to compare human and rat cerebral hemodynamics, as experimental results on rats can only be extrapolated to humans and finally to the clinical management of patients, if the experimental system and human physiology and pathophysiology are comparable not only with respect to outcome related endpoints but also with respect to the dynamics of the regulatory systems involved.

The analysis of both models has shown that there are different nonlinear phenomena in the rat and in the human model.

If physiological parameters are set to values which are typically seen in patients that suffer from TBI in combination with hemodynamic instability, *i.e.* lowered blood pressure combined with intracranial hypertension, the human model displays periodic behaviour while the rat model shows stationary solutions only.

In terms of the clinical conditions this means that in the human model dangerous differences in intracranial pressure occur, while the rat model does not display these sudden changes in intracranial pressure. As a matter of fact there is good clinical evidence concerning the occurrence of plateau waves in humans, while there is no evidence documenting the existence of plateau waves in rat models of TBI or in models of TBI combined with hemodynamic instability.

From the physiological point of view the rat model can be assumed to be more robust compared to the human model. This is an observation which can be agreed upon, although only on the phenomenological level in the first instance, if the clinical performance of humans and rats is compared.

Corresponding to the results of earlier works (cf. [19,21]) the analysis of our human model suggests that the origination of intracranial plateau waves is triggered by either a critical vasodilatory stimulus or a dysbalance between intracranial fluid extravasation and reabsorption.

These results suggest a significant difference between the human system and the animal system in terms of the dynamic response in certain clinical situations. As this phenomenon is especially interesting with respect to the clinically important secondary brain damage problem, further analysis is required to discover whether this observation reflects a true difference of the systems under investigation or whether it is a structural epiphenomenon resulting from the model structure.

References

[1] Maegele, M., Riess, P., Sauerland, S., Bouillon, B., Hess, S., McIntosh, T.K., Mautes, A., Brockmann, M., Koebke, J., Knifka, J. and Neugebauer, E.A., 2005, Characterization of a new rat model of experimental combined neurotrauma, *Shock*, **23**(5), 476–481.

[2] Riess, P., Zhang, C., Saatman, K.E., Laurer, H.L., Longhi, L.G., Raghupathi, R., Lenzlinger, P.M., Lifshitz, J., Boockvar, J., Neugebauer, E., Snyder, E.Y. and McIntosh, T.K., 2002, Transplanted neural stem cells survive, differentiate, and improve neurological motor function after experimental traumatic brain injury, *Neurosurgery*, **51**(4), 1043–1052.

[3] Daun, S. and Tjardes, T., 2005, Development of a species-specific model of cerebral hemodynamics, *Journal of Theoretical Medicine*, **6**(3), 181–195.

[4] Waschke, K.F., Riedel, M., Lenz, C., Albrecht, D.M., von Ackern, K. and Kuschinsky, W., 2004, Regional heterogeneity of cerebral blood flow response to graded pressure-controlled hemorrhage, *The Journal of Trauma*, **56**, 591–603.

[5] Ursino, M., Ter Minassian, A., Lodi, C.A. and Beydon, L., 2000, Cerebral hemodynamics during arterial and CO_2 pressure changes: *in vivo* prediction by a mathematical model, *American Journal of Physiology Heart and Circulatory Physiology*, **279**, H2439–H2455.

[6] Ursino, M. and Lodi, C.A., 1998, Interaction among autoregulation, CO_2 reactivity, and intracranial pressure: a mathematical model, *American Journal of Physiology Heart and Circulatory Physiology*, **274**, H1715–H1728.

[7] Gotoh, T.M., Fujiki, N., Tanaka, K., Matsuda, T., Gao, S. and Morita, H., 2004, Acute hemodynamic responses in the head during microgravity induced by free drop in anesthetized rats, *American Journal of Physiology Heart and Circulatory Physiology*, **286**, R1063–R1068.

[8] Baumbach, G.L., 1996, Effects of increased pulse pressure on cerebral arterioles, *Hypertension*, **27**, 159–167.

[9] Sugiyama, T., Kawamura, K., Nanjo, H., Sageshima, M. and Masuda, H., 1997, Loss of arterial dilation in the reendothelialized area of the flow-loaded rat common carotid artery, *Arteriosclerosis, Thrombosis, and Vascular Biology*, **17**, 3083–3091.

[10] Holtzer, S., Vigue, B., Ract, C., Samii, K. and Escourrou, P., 2001, Hypoxia-hypotension decreases pressor responsiveness to exogenous catecholamines after severe traumatic brain injury in rats, *Critical Care Medicine*, **29**(8), 1609–1614.

[11] Hoppensteadt, F.C. and Peskin, C.S., 2004, Modeling and simulation in medicine and the life sciences. *Texts in Applied Mathematics*, 10th ed. (New York: Springer Verlag).

[12] McGavock, J.M., Mandic, S., Lewanczuk, R., Koller, M., Vondermuhl, I., Quinney, A., Taylor, D., Welsh, R. and Haykowsky, M., Cardiovascular adaptations to exercise training in postmenopausal women with type 2 diabetes mellitus, Department of Physiology, University of Alberta, Edmonton, AB, http://www.epicore.ualberta.ca/pdf%20files/CSRD2004Abstracts.pdf, page existed at 11/21/05.

[13] Vaughn, M.W., Kuo, L. and Liao, J.C., 1998, Estimation of nitric oxide production and reaction rates in tissue by use of a mathematical model, *The American Journal of Physiology*, **274**, H2163–H2176.

[14] Mokrane, A. and Nadeau, R., 1998, Dynamics of heart rate response to sympathetic nerve stimulation, *The American Journal of Physiology*, **275**, H995–H1001.

[15] Harper, A.M. and Glass, H.I., 1965, Effect of alterations in the arterial carbon dioxide tension on the blood flow through the cerebral cortex at normal and low arterial blood pressure, *Journal of Neurology, Neurosurgery, and Psychiatry*, **28**, 449–452.

[16] Kavdia, M., Tsoukias, N.M. and Popel, A.S., 2002, Model of nitric oxide diffusion in an arteriole: impact of hemoglobin-based blood substitutes, *American Journal of Physiology Heart and Circulatory Physiology*, **282**, H2245–H2253.

[17] Seydel, R., 1994, *Practical Bifurcation and Stability Analysis* (New York: Auflage Springer-Verlag), **2**.

[18] Kuznetsov, Y.A., 1998, *Elements of Applied Bifurcation Theory* (New York: Auflage Springer-Verlag), **2**.

[19] Ursino, M. and Lodi, C.A., 1997, A simple mathematical model of the interaction between intracranial pressure and cerebral hemodynamics, *Journal of Applied Physiology*, **82**(4), 1256–1269.

[20] Risberg, J., Lundberg, N. and Ingvar, D.H., 1969, Regional cerebral blood volume during acute transient rises of the intracranial pressure (plateau waves), *Journal of Neurosurgery*, **31**, 303–310.

[21] Rosner, M.J. and Becker, D.P., 1984, Origin and Evolution of plateau waves. Experimental observations and a theoretical model, *Journal of Neurosurgery*, **60**(2), 312–324.

[22] Stevens, S.A., Lakin, W.D. and Goetz, W., 2003, A differentiable, periodic function for pulsatile cardiac output based on heart rate and stroke volume, *Mathematical Biosciences*, **182**(2), 201–211.

Appendix A

All model equations are presented in Appendix A.

A.1 Extracranial arterial pathways

The work of Ursino *et al.* [5] is used as the basic model for the new investigations. There only the cerebral hemodynamics are considered and the blood pressure P_a is chosen as a constant input parameter for the cerebral blood circulation. In this work the extracranial arterial pathways are also modelled and thus the arterial blood pressure is no constant parameter but depends on time t, cardiac output Q and thus on cardiac parameters.

Changes in blood pressure dP_a/dt are described by the following differential equation

$$\frac{dP_a}{dt} = \frac{1}{C_a}\left(Q - \frac{P_a}{R_s}\right), \qquad (A-1)$$

where C_a is the aortic compliance and R_s the systemic resistance. The fraction of cardiac output Q which goes into the head is then given by $(P_a - P_{la})/R_{la}$, where P_{la} and R_{la} are pressure and resistance of the large and middle cerebral arteries, respectively.

A.2 Cardiac output

The model function for cardiac output Q, developed by Stevens *et al.* [22], is used to get a pulsatile blood flow throughout the circulatory system.

The cardiac output Q is modelled by defining an interior function which oscillates with the frequency of the heart pulse and an envelope function for these interior oscillations. By normalizing the product of these functions so that the total outflow over one period equals the stroke volume ν one gets

$$Q(t, n, \Phi) = \frac{\nu}{A(n, \Phi)} \sin^n(\omega t) \cos(\omega t - \Phi) \qquad (A-2)$$

where

$$A(n, \Phi) = \int_0^p \sin^n(\omega t) \cos(\omega t - \Phi) dt, \qquad (A-3)$$

and t is time, ω one half of the basic frequency of the heart pulse, p the period of the heart cycle, Φ a suitable phase angle and n determines the narrowness of the output function Q.

A.3 Intracranial hemodynamics and hydrodynamics

In this model, volume changes in the craniospinal space are ascribed to four compartments: large and middle cerebral arteries dV_{la}/dt, pial arteries and arterioles dV_{pa}/dt, cerebral veins dV_v/dt, and the H_2O compartment dV_{H_2O}/dt, where the H_2O compartment is modelled similar to the CSF compartment in Ref. [5]. According to the Monro–Kellie doctrine the following conservation equation holds:

$$C_{ic} \frac{dP_{ic}}{dt} = \frac{dV_{la}}{dt} + \frac{dV_{pa}}{dt} + \frac{dV_v}{dt} + \frac{dV_{H_2O}}{dt} \qquad (A-4)$$

with time t.

Changes in volume in the H_2O compartment are given by $dV_{H_2O}/dt = q_f - q_o$, where q_f and q_o represent water or cerebrospinal fluid flow into and out of the craniospinal space, respectively. Because both processes are assumed to be passive and unidirectional, we have

$$q_f = \begin{cases} \frac{P_c - P_{ic}}{R_f} & \text{if } P_c > P_{ic} \\ 0 & \text{else} \end{cases} \qquad (A-5)$$

$$q_o = \begin{cases} \frac{P_{ic} - P_{vs}}{R_o} & \text{if } P_{ic} > P_{vs} \\ 0 & \text{else.} \end{cases} \qquad (A-6)$$

where R_f and R_o are inflow and outflow resistances, respectively. P_c is cerebral capillary pressure and P_{vs} is dural sinus pressure.

The intracranial compliance C_{ic}, which represents the capacity of the craniospinal system to store a volume load, is according to Ref. [5] assumed to be inversely proportional to intracranial pressure through a constant parameter

$$C_{ic} = \frac{1}{k_E \times P_{ic}} \tag{A-7}$$

where k_E is the intracranial elastance coefficient.

The first intracranial segment of the model represents the circulation of blood in the large and middle cerebral arteries. The hemodynamic is described by a hydraulic resistance R_{la} and a hydraulic compliance C_{la}. In contrast to the model of Ref. [5] changes in the storage capacity C_{la} and thus on the blood volume V_{la} and the pressure P_{la} are modelled.

The pressure changes dP_{la}/dt in the large and middle cerebral arteries are described by the following differential equation

$$\frac{dP_{la}}{dt} = \frac{1}{C_{la}} \left(\frac{P_a - P_{la}}{R_{la}} - \frac{P_{la} - P_{pa}}{R_{pa}/2} \right) + \frac{dP_{ic}}{dt} \tag{A-8}$$

where P_{la}, P_{pa} and R_{la}, R_{pa} are pressures and hydraulic resistances of the large and middle cerebral arteries and the pial arterial–arteriolar vascular bed, respectively.

The compliance C_{la} of these large cerebral vessels is assumed to be inversely proportional to the transmural pressure

$$C_{la} = \frac{k_{C_{la}}}{P_{la} - P_{ic}} \tag{A-9}$$

with $k_{C_{la}}$ the proportionality constant.

In the pial arterial compartment all sections of the cerebrovascular bed directly under the control of the regulatory mechanisms are comprised. This pial arterial segment is described by a hydraulic resistance R_{pa} and a hydraulic compliance C_{pa}. Both of these parameters are regulated by cerebrovascular control mechanisms. The two equations which describe the changes in volume dV_{pa}/dt in this segment and the calculation of the pressure at the cerebral capillaries P_c (applying Kirchhoff's law) are given in Ref. [5].

With these three equations the pressure change dP_{pa}/dt in the pial arterial compartment is described by

$$\frac{dP_{pa}}{dt} = \frac{1}{C_{pa}} \left[\frac{P_{la} - P_{pa}}{R_{pa}/2} - \frac{P_{pa} - P_c}{R_{pa}/2} - \frac{dC_{pa}}{dt}(P_{pa} - P_{ic}) \right] + \frac{dP_{ic}}{dt}. \tag{A-10}$$

The intracranial vascular bed of the veins is described by a series arrangement of two segments. The first, from the small postcapillary venules to the large cerebral veins, contains the resistance R_{pv} and the venous compliance C_{vi}. Corresponding to Ref. [5] the compliance is calculated by

$$C_{vi} = \frac{k_{ven}}{P_v - P_{ic} - P_{v1}}, \tag{A-11}$$

where k_{ven} is a constant parameter and P_{v1} represents the transmural pressure value at which cerebral veins collapse.

Using the equations defined in Ref. [5], which describe the volume changes $\mathrm{d}V_{\mathrm{v}}/\mathrm{d}t$ of this venous compartment, the pressure changes $\mathrm{d}P_{\mathrm{v}}/\mathrm{d}t$ are given by

$$\frac{\mathrm{d}P_{\mathrm{v}}}{\mathrm{d}t} = \frac{1}{C_{\mathrm{vi}}}\left(\frac{P_{\mathrm{c}} - P_{\mathrm{v}}}{R_{\mathrm{pv}}} - \frac{P_{\mathrm{v}} - P_{\mathrm{vs}}}{R_{\mathrm{vs}}}\right) + \frac{\mathrm{d}P_{\mathrm{ic}}}{\mathrm{d}t}, \qquad (\mathrm{A} - 12)$$

where R_{vs} is the resistance of the terminal intracranial veins and P_{vs} the pressure at the dural sinuses.

The second segment represents the terminal intracranial veins (*e.g.* lateral lakes). During intracranial hypertension these vessels collide or narrow at their entrance into the dural sinuses, with a mechanism similar to that of a starling resistor (cf. [5]). Because of this phenomenon the resistance R_{vs} depends on the pressures of the system in the following way:

$$R_{\mathrm{vs}} = \frac{P_{\mathrm{v}} - P_{\mathrm{vs}}}{P_{\mathrm{v}} - P_{\mathrm{ic}}} R_{\mathrm{vs1}}, \qquad (\mathrm{A} - 13)$$

where R_{vs1} represents the terminal vein resistance when $P_{\mathrm{ic}} = P_{\mathrm{vs}}$.

In contrast to the model of Ref. [5] the sinus venous pressure P_{vs} is not assumed to be constant, but depends on time and the other pressures of the system and is calculated by Kirchhoff's law

$$\frac{P_{\mathrm{v}} - P_{\mathrm{vs}}}{R_{\mathrm{vs}}} + q_{\mathrm{o}} = \frac{P_{\mathrm{vs}} - P_{\mathrm{cv}}}{R_{\mathrm{ve}}}. \qquad (\mathrm{A} - 14)$$

Since the water backflow at the dural sinuses q_{o} is negligible in comparison to the blood flows, it is assumed to be zero.

The extracranial venous circulation from the dural sinuses through the vena cava back to the heart is described by the hydraulic resistance R_{ve} and the hydraulic compliance C_{ve}. Because no mechanisms acting on these blood vessels are taken into account, these parameters are assumed to be constant.

A.4 Cerebrovascular regulation mechanisms

Cerebrovascular regulation mechanisms work by modifying the resistance R_{pa} and the compliance C_{pa} (and hence the blood volume) in the pial arterial–arteriolar vasculature.

In this section three mechanisms are considered which regulate cerebral blood flow. The effects of two of them, like autoregulation and CO_2 reactivity, are described in Ref. [5]. One new cerebrovascular regulation mechanism, the NO reactivity, is inserted into the model and its effect on the pial arterial compliance is modelled by using the given idea in Ref. [5] of a sigmoidal relationship of the whole regulation process.

The actions of the cerebrovascular regulation mechanisms are described by means of a first order low pass filter with time constant τ_{aut}, $\tau_{\mathrm{CO_2}}$ and τ_{NO} and gains G_{aut}, $G_{\mathrm{CO_2}}$ and G_{NO}.

This corresponds to the following differential equations

$$\frac{dx_{\text{aut}}}{dt} = \frac{1}{\tau_{\text{aut}}}\left[-x_{\text{aut}} + G_{\text{aut}}\frac{q - q_n}{q_n}\right] \qquad (A - 15)$$

$$\frac{dx_{CO_2}}{dt} = \frac{1}{\tau_{CO_2}}\left[-x_{CO_2} + G_{CO_2}A_{CO_2}\log_{10}\left(\frac{P_{aCO_2}}{P_{aCO_2n}}\right)\right] \qquad (A - 16)$$

$$\frac{dx_{NO}}{dt} = \frac{1}{\tau_{NO}}\left[-x_{NO} + G_{NO}\log_{10}\left(\frac{q_{NO}}{q_{NOn}}\right)\right], \qquad (A - 17)$$

where x_{aut}, x_{CO_2} and x_{NO} are state variables of the model that account for the effects of autoregulation, CO_2 and NO reactivity, respectively. q_n, P_{aCO_2n} and q_{NOn} are set points for the regulatory mechanisms. The cerebral blood flow q is calculated by Ohm's law:

$$q = \frac{P_{\text{pa}} - P_{\text{c}}}{R_{\text{pa}}/2}. \qquad (A - 18)$$

The strength of the CO_2 reactivity in the model is not constant but decreases during severe ischemia. This phenomenon is described by the corrective factor A_{CO_2} in equation (A-16) which has the following expression

$$A_{CO_2} = \frac{1}{1 + \exp\{[-k_{CO_2}(q - q_n)/q_n] - b_{CO_2}\}} \qquad (A - 19)$$

with constant parameters k_{CO_2} and b_{CO_2} (cf. [5]).

Finally, by adapting the situation of Ref. [5] to three regulation mechanisms one gets the value of the pial arterial compliance depending on x_{aut}, x_{CO_2} and x_{NO}

$$C_{\text{pa}} = \frac{(C_{\text{pan}} - \Delta C_{\text{pa}}/2) + (C_{\text{pan}} + \Delta C_{\text{pa}}/2)\exp[(x_{CO_2} + x_{NO} - x_{\text{aut}})/k_{C_{\text{pa}}}]}{1 + \exp[(x_{CO_2} + x_{NO} - x_{\text{aut}})/k_{C_{\text{pa}}}]} \qquad (A - 20)$$

where C_{pan} is the pial arterial compliance under basal conditions, ΔC_{pa} the change in compliance and $k_{C_{\text{pa}}}$ a constant parameter, which is chosen in the way that the slope of the sigmoidal curve at $C_{\text{pa}} = C_{\text{pan}}$ is equal to 1. This condition is satisfied by choosing $k_{C_{\text{pa}}} = \Delta C_{\text{pa}}/4$.

An important point is that this sigmoidal curve is not symmetrical: the increase in blood volume caused by vasodilation is greater than the decrease of blood volume caused by vasoconstriction. That is the reason why two different values of the parameter ΔC_{pa} have to be chosen depending on whether vasodilation or vasoconstriction is considered. It is

$$\begin{cases} x_{CO_2} + x_{NO} - x_{\text{aut}} > 0 : \Delta C_{\text{pa}} = \Delta C_{\text{pa1}}; k_{C_{\text{pa}}} = \Delta C_{\text{pa1}}/4 \\ x_{CO_2} + x_{NO} - x_{\text{aut}} < 0 : \Delta C_{\text{pa}} = \Delta C_{\text{pa2}}; k_{C_{\text{pa}}} = \Delta C_{\text{pa2}}/4. \end{cases} \qquad (A - 21)$$

An expression for dC_{pa}/dt is obtained by differentiating equation (C_{pa}) to

$$\frac{dC_{pa}}{dt} = \frac{\Delta C_{pa}}{k_{C_{pa}}} \frac{\exp[(x_{CO_2} + x_{NO} - x_{aut})/k_{C_{pa}}]}{\{1 + \exp[(x_{CO_2} + x_{NO} - x_{aut})/k_{C_{pa}}]\}^2} \times \frac{d(x_{CO_2} + x_{NO} - x_{aut})}{dt}. \qquad (A-22)$$

The cerebrovascular control mechanisms act also on the hydraulic pial arterial resistance R_{pa}. Because the blood volume is directly proportional to the inner radius second power, while the resistance is inversely proportional to inner radius forth power, the following relationship holds between the pial arterial volume and resistance (cf. [5])

$$R_{pa} = \frac{k_R C_{pan}^2}{V_{pa}^2} \qquad (A-23)$$

where k_R is a constant parameter.

A.5 Release of norepinephrine and its impact on heart rate

The changes of the norepinephrine concentration in blood $d[NE]/dt$ are described by the equation

$$\frac{d[NE]}{dt} = r - \alpha_{NE}[NE], \qquad (A-24)$$

where r is the constant NE release during sympathetic nerve stimulation and α_{NE} is the NE elimination rate.

The heart rate response to a steplike increase of the norepinephrine concentration [NE] is described by

$$\tau_{hr} \frac{dhr}{dt} = -hr + G([NE]), \qquad (A-25)$$

where hr is the heart rate variation. The steady-state heart rate response $G([NE])$ is, according to [14], defined by

$$\Delta HR = G([NE]) = \frac{\Delta HR_{max}[NE]^2}{k_{NE}^2 + [NE]^2}, \qquad (A-26)$$

where K_{NE} is the NE concentration producing a half maximum response and ΔHR_{max} is the maximum value of ΔHR.

The new heart rate $\bar{b}$ is then given by adding the heart rate variation hr to b.